



Published in final edited form as:

Mucosal Immunol. 2020 March ; 13(2): 371–380. doi:10.1038/s41385-019-0234-5.

Type I IFN ineffectively activates neonatal dendritic cells limiting respiratory antiviral T cell responses

Annie W. Lau-Kilby¹, Mathilde Turfkruyer¹, Margaret Kehl¹, Lijuan Yang², Ursula J. Buchholz², Kimberly Hickey³, Allison M.W. Malloy¹

¹Laboratory of Infectious Diseases and Host Defense, Department of Pediatrics, F. Edward Hébert School of Medicine, Uniformed Services University of the Health Sciences, 4301 Jones Bridge Road, Bethesda, MD 20814, USA

²RNA Viruses Section, Laboratory of Infectious Diseases, NIAID, NIH, Bldg. 50, Rm 6503, 50 South Drive, MSC 8007, Bethesda, MD 20892

³Department of Obstetrics and Gynecology, Walter Reed National Military Medical Center, 8901 Wisconsin Avenue, Bethesda, MD 20889

Abstract

Insufficient T cell responses contribute to the increased burden of viral respiratory disease in infancy. Neonatal dendritic cells (DCs) often provide defective activation of pathogen-specific T cells through mechanisms that are incompletely understood, which hinders vaccine design for this vulnerable age group. Enhancing our characterization of neonatal DC sub-specialization and function is therefore critical to developing their potential for immunomodulation of T cell responses. In this study, we engineered respiratory syncytial virus (RSV) to express a model protein, ovalbumin, to track antigen-presenting DCs *in vivo*. We found that murine neonatal conventional DC1s (cDC1s) efficiently migrated and presented RSV-derived antigen, challenging the paradigm that neonatal DCs are globally immature. In a key observation, however, we discovered that during infection neonatal cDC1s presenting viral antigen were unable to upregulate costimulatory molecules in response to type I interferons (IFN-I), contributing to poor antiviral T cell responses. Importantly, we showed that the deficient response to IFN-I was also exhibited by human neonatal cDC1s, independent of infection. These findings reveal a functionally distinct response to IFN-I by neonatal cDC1s that may leave young infants susceptible to viral infections, and provide a new target for exploration, in light of failed efforts to design neonatal RSV vaccines.

Users may view, print, copy, and download text and data-mine the content in such documents, for the purposes of academic research, subject always to the full Conditions of use:http://www.nature.com/authors/editorial_policies/license.html#terms

Corresponding author: A. Malloy (Allison.malloy@usuhs.edu).

AUTHOR CONTRIBUTIONS

A.W.L-K and A.M.W.M. conceived the project and designed the experiments; A.W.L-K, M. T-H., M. K., and A.M.W.M. conducted the experiments; A.W.L-K. performed formal analysis; A.W.L-K and A.M.W.M. wrote the original manuscript and all authors contributed to the writing and editing of the manuscript; L.Y., U.B. and K. M provided resources; Funding was acquired by A.M.W.M.

Potential conflicts of interest: U.J.B is listed as an inventor on a patent application for genetically stable live-attenuated RSV vaccines. All other authors report no potential conflicts of interest.

ADDITIONAL INFORMATION

The online version of this article contains supplementary material, which is available to authorized users.

INTRODUCTION

Immune responses evolve with aging.¹ During the neonatal period, age-dependent immunity facilitates *in utero* demands of protecting the developing fetus,² and after birth, enables microbial colonization of the skin and mucosal surfaces.³ Furthermore, restrictions on inflammation protect the developing neonatal lung for air exchange.⁴ These requirements of early life dampen innate immune responses to invading pathogens and reduce pathogen-specific adaptive responses,^{5, 6} contributing to the increased burden of respiratory infections in young infants. Globally, respiratory tract infections are the primary cause of mortality during the first year of life, with RSV contributing to the majority of these deaths.⁷ Nearly all children have been exposed to RSV by 2 years of age, yet reinfection throughout life is common,⁸ suggesting that early life infection fails to generate durable protective immunity. Identifying innate immune regulation that influences the outcome of protective antiviral T cell responses^{9–11} during infancy is therefore critical to much needed vaccine design.

cDCs are key components of the innate immune response that determine the magnitude and function of antiviral T cell responses.¹² DCs perform distinct non-redundant roles through sub-specialization: CD103⁺ cDCs (cDC1s) specialize in cross-presentation of class I major histocompatibility complex (MHC-I) restricted antigens to CD8⁺ T cells, whereas CD11b⁺ cDCs (cDC2s) more frequently present antigen to CD4⁺ T cells. In the lungs, cDCs insert dendrites through the respiratory epithelium, sensing for danger signals in the airways, and taking up antigens for processing and presentation. Once activated, cDCs rapidly migrate to the lung draining lymph node (dLN) to engage naïve antigen-specific T cells. This engagement is most critical in neonates, because they have not yet encountered the majority of pathogens. However, current knowledge of DC ontogeny and activation predominantly comes from studies in adults,^{13, 14} and less is known about the function of DC subsets in early life. Recent studies suggest T cell activation by murine neonatal cDCs differs from adults' during viral respiratory infections and allergic responses due to impaired antigen-presentation and responsiveness to cytokine cues.^{15–17} The inability to track DCs presenting antigens of interest *in vivo* has prevented further assessment of their age-dependent functions that determine the quality of T cell responses.

By engineering RSV to express the full-length ovalbumin protein (RSV-ova), we were able, for the first time, to track antigen-presenting respiratory DCs in neonatal and adult mice during infection and evaluate their effect on antigen-specific T cell responses. Using this new model, we discovered that neonatal cDC1s effectively processed and presented the MHC-I, H-2K^b, restricted epitope, SIINFEKL_(257–264), (K^b-OVA) during a respiratory infection with RSV-ova and transported this antigen to the dLN for T cell priming. Unexpectedly, despite presenting virus-derived antigen, neonatal cDC1s failed to upregulate costimulatory molecules leading to reduced neonatal OVA_{257–264}-specific CD8⁺ T cell responses. To uncover the defect in activation during infection, the transcriptional responses of adult and neonatal K^b-OVA⁺ cDC1s were compared, which identified reduced expression of interferon signaling genes in neonates. In contrast to adults, *in vivo* treatment with IFN-I could not induce costimulatory molecule expression by neonatal cDC1s, identifying a defect in their responsiveness to this antiviral cytokine. Through detailed analysis of DC subsets in human umbilical cord blood, we also demonstrated a parallel defect in the ability of human

neonatal cDC1s to respond to IFN-I. Together these findings identified an age-dependent cDC1-specific response to IFN-I that accounted for poor antiviral T cell responses in neonates and can be targeted by vaccine design to increase the precision of T cells.

RESULTS

RSV-ova is an effective tool for tracking antigen processing and presentation *in vivo*

Our understanding of DC subsets and their function continues to evolve as new phenotypic markers and transcriptional regulators are identified.¹⁸ However, further characterization of DC function that determines the outcome of T cell responses requires improved *in vivo* tracking of DCs presenting specific antigen(s) of interest. Reporter viruses, such as influenza-expressing green fluorescent protein (PR8-gfp), have been used to detect infected DCs presumed to be directly presenting antigens.¹⁹ Previously, we reported that fewer than 1% of DCs migrating to the dLN are GFP⁺ after RSV-gfp infection, suggesting migratory DCs may primarily cross-present RSV antigens.¹⁵ To track DCs cross-presenting RSV-derived antigen during *in vivo* infection, we generated RSV-ova, a recombinant virus expressing the full-length chicken ovalbumin protein (OVA) from an additional gene inserted between the RSV G and F proteins (Supplemental Fig. 1a). Following intranasal infection, RSV-ova replication in the lungs did not significantly differ between age groups, and was attenuated compared to unmodified RSV A2 (RSV-wt) (Supplemental Fig. 1b, c). The number of RSV-specific CD8⁺ T cells, recognizing epitopes in the M2 (M2₈₂₋₉₀) and M (M₁₈₇₋₁₉₅) proteins, was similar between the two viruses (Supplemental Fig. 1d) indicating that the difference in the level of viral replication did not affect the magnitude of the T cell responses, consistent with our previously published findings.¹⁶

Next, we tested the binding of the anti-K^b-OVA antibody (clone 25D1.16²⁰) using peptide-loaded CB6F1/J splenocytes and confirmed the peptide and MHC haplotype specificity of this antibody (Supplemental Fig. 1e, f). Upon intranasal RSV-ova infection, respiratory DCs presenting the SIINFEK epitope from ovalbumin in the context of H-2K^b were recognized by two anti-K^b-OVA antibodies with the same specificity conjugated to different fluorochromes. DCs from RSV-wt infected mice were used as a negative control to confirm K^b-OVA staining (Supplemental Fig. 1g-j). We implemented this method, which has been used by others, to increase the specificity for rare cell identification²¹. Together, these data demonstrate that RSV-ova is an effective tool to track antigen presentation *in vivo* and for evaluating the interplay between DCs and T cells.

Neonatal cDC1s efficiently present RSV-derived MHC-I restricted antigen during infection

Using the validated RSV-ova model and staining panel, we initially characterized the influx of cDC1, cDC2, and pDC subsets into the dLN, regardless of antigen presentation (Fig. 1a, b). Neonatal cDC1s represented a greater percentage of the DCs in the dLN compared to adults (Fig. 1a, b, *green*), which is consistent with RSV-wt infection.¹⁵ We found that the majority of RSV-derived K^b-OVA was presented by cDC1s in both age groups, however, a higher proportion of neonatal cDC1s expressed K^b-OVA⁺ (Fig. 1b, c, *green*). cDC2s presented K^b-OVA, although at significantly lower levels than cDC1s (Fig. 1b, *blue*). pDCs did not exhibit measurable anti-K^b-OVA binding (Fig. 1b, c, *maroon*). Quantification of the

average abundance of K^b-OVA expression per cell, as measured by mean fluorescence intensity (MFI), showed that adult and neonatal presentation on cDC1s was similar (Supplemental Fig. 1k).

To further evaluate the ability of neonatal and adult cDC1s to process and present antigen during a viral respiratory infection, we measured the proliferation of ova-specific T cell receptor (TCR) transgenic CD8⁺ T cells (OT-I tg cells) after culture with cDC1s that acquired antigen *in vivo* during RSV-ova infection. Total cDC1s were sorted from the dLNs of RSV-ova infected mice at 2 DPI and co-cultured with CFSE-labeled OT-I tg cells. Proliferation, measured by CFSE dilution from OT-I tg cell division, was similar between OT-I tg cells exposed to neonatal or adult cDC1s from infected mice (Fig. 1d, f). OT-I tg cells are highly sensitive to their cognate antigen, SIINFEKL, with limited requirements for second and third signaling to induce proliferation as shown by others^{22, 23} and in Fig. 1e. This system, therefore, provides a measurement of antigen availability and further establishes the similar competence of neonatal and adult cDC1s to process and present antigen for TCR engagement.

In summary, we have shown, by *in vivo* expression and *in vitro* function, that the cDC1 subset is superior at presenting K^b-OVA acquired during *in vivo* RSV-ova infection in both adults and neonates; and that neonatal cDC1s did not exhibit a defect in MHC-I antigen-presentation compared to adult cDC1s.

Despite effective antigen presentation, the magnitude of the neonatal CD8⁺ T cell response is diminished

The amount of presented antigen has been suggested to correlate with the frequency of antigen-specific T cells,^{24, 25} however, *in vivo* antigen presentation has been difficult to quantify. Our previous studies were unable to measure the *in vivo* MHC-I restricted presentation of the RSV epitopes, K^d-M₂₈₂₋₉₀ and D^b-M₁₈₇₋₁₉₅^{15, 16, 26}. We, therefore, could not determine if defective neonatal antigen presentation contributed to reduced neonatal antiviral CD8⁺ T cell responses (Fig. 2a, b), as suggested by other reports^{27, 28}. Using RSV-ova, we were able to directly compare antigen presentation (K^b-OVA) with the frequency of responding T cells. Surprisingly, despite similarly effective K^b-OVA presentation by cDC1s in both adults and neonates (Fig. 1b, c), the OVA₂₅₇₋₂₆₄-specific (OVA-specific) CD8⁺ T cell response was diminished in neonates (Fig. 2a, b). These data showed that neonates induced limited anti-RSV OVA-specific CD8⁺ T cell responses that were not due to the lack of cognate antigen presented.

In neonates, dysfunctional activation of K^b-OVA⁺ cDC1s impairs anti-RSV-ova CD8⁺ T cell responses

In addition to antigen presentation, DCs must upregulate a cascade of activation events for the effective priming of pathogen-specific CD8⁺ T cells including efficient migration to the dLN and expression of costimulatory molecules.²⁹ Now equipped with a method for tracking DCs presenting virus-specific antigen, we next investigated these components of activation. Migration into the T cell zones of lymph nodes is induced by upregulation of CCR7, which binds ligands CCL19 and CCL21 expressed by lymphatic vessels and T cell

zones in lymph nodes.¹³ We found that neonatal K^b-OVA⁺ cDC1s exhibited enhanced expression of CCR7 compared to adults (Fig. 2c), suggesting their migratory potential to reach naïve T cells in the dLN surpassed that of adults, and may have contributed to the higher frequency of neonatal K^b-OVA⁺ cDC1s in the dLN 2 DPI (Fig. 1c).

Costimulation by cDCs supports TCR engagement promoting T cell activation and proliferation.³⁰ Several costimulatory molecules were measured on entire DC subsets and compared with those expressing K^b-OVA⁺ within the subset to characterize their activation profiles during infection and in the context of antigen presentation. In association with antigen presentation, adult cDC1s dramatically upregulated expression of the critical costimulatory molecule, CD86, in sharp contrast to neonatal K^b-OVA⁺ cDC1s (Fig. 2d *top*, e, f). The age-dependent difference in CD86 upregulation was unexpectedly pronounced when comparing antigen-presenting cDC1s rather than the entire subset (Fig. 2d, *top vs bottom*). Additionally, adult K^b-OVA⁺ cDC1s upregulated CD86 expression by 20-fold at 1 DPI compared to steady-state cDC1s, demonstrating a remarkable ability to upregulate this molecule upon acquisition of RSV-derived antigen, which the neonatal cDC1s did not (Fig. 2e, f). CD80 and CD86 can play compensatory roles during T cell priming, and CD80 also was increased on adult compared to neonatal K^b-OVA⁺ cDC1s (Supplemental Fig. 11). CD40, which supports the DC-T cell dialogue, exhibited a modest increase in MFI on adult compared to neonatal K^b-OVA⁺ cDC1s, which was not observed when comparing the entire cDC1 subset (Supplemental Fig. 11). These data highlight the poor upregulation of costimulation by neonatal K^b-OVA⁺ cDC1s, which was in contrast to their ability to migrate to the dLN, identifying a dysfunction in activation during RSV infection.

To assess the impact of dysfunctional cDC1 activation on the anti-RSV-ova CD8⁺ T cell response, we performed *in vivo* blockade of costimulation in adults. *In vivo* blockade of CD86/80 1 DPI, during the peak of costimulatory molecule expression and T cell priming, reduced the adult OVA-specific CD8⁺ T cell response to neonatal levels (Fig. 2g). Blockade also impaired the M2- and M-specific CD8⁺ T cell responses (Fig. 2g), recapitulating our previous observations.¹⁵ Blockade of CD40 slightly diminished antiviral T cell responses, but did not identify a predominant role for this molecule in the primary anti-RSV-ova CD8⁺ T cell responses (Fig. 2g). Delayed blockade of CD86/80 at 5 DPI did not reduce the OVA-specific CD8⁺ T cell response, confirming the importance of costimulation for T cell priming provided 1 DPI, during peak expression on cDC1s.

Based on these findings, we show that costimulation provided by migratory cDC1s during peak antigen presentation determines the magnitude of the OVA-specific CD8⁺ T cell expansion. By defining a primary defect in costimulation, but sufficient functional antigen presentation and migratory responses, we have constructed a highly relevant model to determine how costimulation is regulated in neonatal cDC1s.

Defects in IFN- γ responsiveness are associated with the dysfunctional activation of neonatal cDC1s during RSV-ova infection

To globally examine the mechanism(s) driving the dysfunctional activation of neonatal cDC1s, we quantified their transcriptional response using RNA-seq. K^b-OVA⁺ enriched cDC1s were sorted from the dLNs at 2 DPI, during the peak of K^b-OVA presentation and

CD86 expression (Fig. 1b, 2d). Pathway analysis of the differentially expressed genes using Ingenuity Pathway Analysis software (IPA)³¹ identified two pathways that were most significantly upregulated in adult compared to neonatal K^b-OVA⁺ cDC1s: dendritic cell maturation and IFN signaling (Supplemental Fig. 2a, b). Furthermore, among the genes associated with the three types of IFN signaling (type I, II, III), those in the IFN-I pathway were most differentially expressed between adult and neonatal K^b-OVA⁺ cDC1s (Fig. 3a).

Early production of innate cytokines, such as IFN-I, contributes to viral control and immune cell activation.¹² To examine the disparity in IFN-I signaling, we next investigated whether neonates produced less IFN-I in response to RSV-ova infection. IFN-I (IFN α / β) was first quantifiable in the lung at 12 hours post-infection. Neonates exhibited reduced production of IFN α / β per lung, and per milligram of tissue (Fig. 3b, c *upper* and *lower*). Delayed IFN α / β production was observed through 18–24 hours post infection in neonates and has been demonstrated in RSV-wt infection by others.³² In addition, lower levels of IFN α were measured in the neonatal compared to the adult dLN (Supplemental Fig. 3a), reflecting reduced cytokine at both the site of cDC activation (lung) and T cell priming (dLN).

Prior reports show that IFN-I upregulates CD86 on antigen presenting cells in adults.³³ To determine if decreased availability of IFN-I in neonates led to the reduced CD86 expression on neonatal K^b-OVA⁺ cDC1s, we proposed to “rescue” this component of activation by administering exogenous IFN-I during neonatal RSV-ova infection. Surprisingly, CD86 expression on neonatal K^b-OVA⁺ cDC1s was not increased after intranasal IFN α treatment (Fig. 3d, *top*), nor was it increased on the total cDC1 (Fig. 3d, *bottom*) and pDC populations (Supplemental Fig. 3d). Neonatal cDC2s exhibited a minimal increase in CD86 expression (Supplemental Fig. 3d). We also observed no significant change in the frequency of anti-RSV-ova-specific CD8⁺ T cell responses after IFN α treatment in neonates (Fig. 3e). We performed similar experiments using IFN β in neonates and again observed no difference in the activation of K^b-OVA⁺ cDC1s (Fig. 3f), nor the magnitude of anti-RSV-ova-specific CD8⁺ T cell responses (Fig. 3g). Even at supraphysiologic doses of IFN β (5000U), we were unable to repair the neonatal response (Supplemental Fig. 3b). Together these data show that the reduced production of IFN-I during RSV infection is not solely responsible for the failure to upregulate CD86 on neonatal K^b-OVA⁺ cDC1s.

The reduced responsiveness to IFN-I in murine neonatal cDC1s is independent of RSV infection

RSV can evade host immunity by directly downregulating the IFN-I response,³⁴ which led us to question whether the dysfunctional cDC1 response to IFN-I in neonates was a result of RSV infection. We therefore asked whether intranasal IFN-I treatment of naive mice could enhance CD86 expression on cDC1s in the lung. While adult cDC1s could upregulate CD86 by 2–3-fold in response to intranasal IFN β , neonatal cDC1s could not (Fig. 4a, b). We also administered IFN β at a 2-fold higher dose in neonates (240 \times 10³ U/g of lung) and still did not observe an increase in CD86 expression (Fig. 4a, b) demonstrating a failure to respond to IFN-I in the absence of RSV infection. Interestingly, neonatal pDCs exhibited increased CD86 expression in response to IFN β (Supplemental Fig. 3e), supporting the findings of others regarding the activation of neonatal pDCs by IFN-I.³² These data indicate that the

ineffective response to IFN-I may be subset-specific. Together these findings show that, neonatal cDC1s can regulate different components of activation independently, and lack of responsiveness to IFN-I impairs their expression of costimulatory molecules, but not antigen presentation or migration.

Human neonatal cDCs also ineffectively respond to IFN-I

Human DC subsets are difficult to study due to their scarcity in peripheral blood. To determine whether human neonatal cDCs also failed to upregulate costimulatory molecules in response to IFN-I, we isolated mononuclear cells (MCs) from human umbilical cord blood (neonate, CBMC) and adult peripheral blood (adult, PBMC) to analyze the cDC subset-specific responses. We stimulated CBMCs and PBMCs directly *ex vivo*, without any *in vitro* derivation, which can alter DC function. Following stimulation, we identified the three different human DC subsets that are equivalent to murine cDC1s, cDC2s, and pDCs by complex flow cytometric analysis (Supplemental Fig. 4).³⁵ Unstimulated neonatal cDC1s and cDC2s trended towards lower levels of CD86 and CD80 compared to adult cells, suggesting that costimulation may be restricted in neonates at baseline (Fig. 5a, b, *top and middle rows*). In response to IFN β stimulation, adult cDC1s and cDC2s efficiently upregulated CD86 and CD80, whereas neonatal cDC subsets demonstrated poor upregulation of these costimulatory molecules (Fig. 5a). Furthermore, the expression level of CD86 and CD80 induced by neonatal cDCs, even at high doses of IFN β , barely reached the level of unstimulated adult cDCs (Fig. 5a, b, c). In contrast, neonatal pDCs responded to IFN-I by upregulating CD80 expression (Fig. 5a, *bottom row*), corroborating our findings in mice and suggesting that the observed defect is cDC-specific.

RSV infection can trigger several toll-like receptors (TLRs). As a single stranded RNA virus, RSV engages TLR 7/8, which can be mimicked by R848.³⁶ Previous studies have shown that R848 stimulation of neonatal immune cells can increase cytokine production and costimulatory molecule expression by APCs.³⁷ Interestingly, we also found that neonatal cDCs lacked the ability to fully upregulate CD86 and CD80 in response to R848 stimulation compared to adult cDCs (Fig. 5a, b, *top and middle rows*). Nonetheless, as with IFN-I stimulation, neonatal pDCs were more responsive to R848 (Fig. 5a, b, *bottom row*).

Consequently, we have shown that the unique cDC-specific response to IFN-I observed in neonatal mice was also exhibited by human neonatal cDCs. These data suggest that RSV may pose specific challenges for neonatal cDCs that are less responsive to the antiviral cytokine, IFN-I, and indicate that cytokines predicted to protect against viral infection in adults may not similarly induce protection in neonates.

DISCUSSION

Neonatal immune responses are predominantly characterized as immature. However, recent findings suggest that immune activation is regulated by distinct requirements of age-dependent development and exposures.^{15, 16, 32, 38, 39} In this report, we counter the paradigm that neonatal DCs are globally immature, by showing that murine neonatal cDC1s responding to RSV infection can effectively present viral antigens and migrate to the site of T cell priming. Despite exhibiting these highly functional maturation responses, they fail to

provide costimulation in response to IFN-I. Importantly, this defective IFN-I response also was apparent in human neonatal cDCs. These data show that IFN-I responsiveness is limited, in a cell-specific manner, during early life, and this limitation of neonatal cDC1 activation reduces virus-specific T cell responses that may increase susceptibility to viral infections.

Poor functional responses of neonatal DCs and T cells have been associated with higher rates of infection in young infants,⁴⁰ but the lack of mechanistic understanding has posed challenges to designing effective vaccines for neonates.⁴¹ Previous reports show conflicting results regarding the ability of neonatal DCs to process and/or present antigen.^{42,15, 28, 43} Our unique model enabled us to track DCs presenting pathogen-associated antigen during a viral respiratory infection and isolate these rare cells for transcriptional analysis. We found that neonatal respiratory cDC1s were effective at presenting antigen derived from RSV-ova and also expressed genes associated with cross-presentation at similar levels to that of adults (Supplemental Fig. 2c) indicating that this component of DC maturation is competent during early life.

In conjunction with antigen presentation, fundamental properties of DC maturation, including migration and T cell costimulation, render DCs superior at activating naïve T cells. In the context of RSV-ova infection, neonatal cDC1s effectively presented pathogen-associated antigen and upregulated CCR7 for migration, but poorly expressed costimulatory molecules. Through tracking K^b-OVA⁺ cells, we uncovered that the defect in CD86 upregulation was most pronounced on neonatal cDC1s presenting antigen. These data establish that maturation, as defined in adult DCs, did not occur in neonatal cDC1s responding to RSV-ova infection, supporting the concept that neonatal immune cells have distinct age-dependent programming rather than global deficits.

While many innate immune stimuli can trigger DC activation, the mechanisms that regulate costimulation are not well defined. Our model enabled us to analyze the transcriptional responses of cDC1s, known to be presenting pathogen-derived antigen, yet expressing different levels of costimulatory molecules. Decreased interferon signaling in neonatal compared to adult K^b-OVA⁺ cDC1s was highlighted by this analysis. IFN-I play a key role in host protection against viruses by impairing viral replication and, importantly, enhancing immune responses.⁴⁴ RSV has uniquely evolved to produce two non-structural genes, NS1 and NS2, that evade IFN-I by antagonizing IFN-stimulated genes and disrupting DC function.^{12, 34} Abrogation of IFN by RSV has been associated with decreased production in the respiratory tract of neonatal mice and human infants.^{32,45} Previously, the administration of exogenous intranasal IFN-I was shown to enhance pDC function and RSV-specific IgA responses in neonatal mice.^{32, 38} Based on these and other reports, it was presumed that limited production and evasion of IFN-I by RSV led to diminished activation of innate immune responses in young infants. In contrast to this prevailing notion, we showed that, compared to adult cDC1s, neonatal cDC1s exhibited reduced responsiveness to IFN-I independent of RSV infection, which led to reduced expression of costimulatory molecules.

A key finding of our study is that age-dependent IFN-I activation of cDC subsets is common to both mice and humans. Human neonatal DCs have been examined primarily from

umbilical cord blood after *in vitro* differentiation into monocyte-derived DCs. These studies have shown reduced cytokine production and costimulatory molecule expression in response to pathogen-associated molecular patterns compared to adult peripheral blood-derived DCs.⁴⁶ We studied human adult peripheral blood and umbilical cord blood DC subsets, without derivation, and showed that human neonatal cDC1s and cDC2s displayed reduced CD86/80 upregulation after IFN-I stimulation. It is interesting to consider why IFN-I may be distinctly regulated during early life: cDCs play critical roles in the establishment of tolerance to self-associated antigen, limiting autoimmunity.^{47, 48} In addition, prominent interferon-response-gene signatures in early life are linked to developmental delays.^{49, 50} Restricted IFN-I responsiveness may, therefore, subvert disruption of early life development. Our findings warrant further investigation into DC responses later in neonatal life given that DCs from umbilical cord blood represent a distinct timepoint in neonatal immune development.

In conclusion, our findings identified a tightly regulated response by cDC1s in the lungs during the neonatal period, and an age-dependent programming that is highly functional in terms of antigen presentation and migration, but limits T cell activation through poor costimulation. During the neonatal period, when tissue development and microbial colonization is ongoing, this programming may prevent destructive inflammation. However, in the context of a viral respiratory infection, this results in reduced pathogen-specific CD8⁺ T cell responses that are important for viral clearance.¹¹ The lack of effective vaccines for neonates, particularly against pathogens that infect the respiratory tract, highlights the importance of defining distinct mechanisms that regulate the development of protective adaptive immune responses. Our findings identify MHC-I antigen presentation as a function of neonatal cDC1s that could be capitalized upon for vaccine design, while costimulation presents a challenge that requires further investigation for infants.

MATERIALS AND METHODS

Mice

Adult (6–10 weeks old) female CB6F1/J mice or OT-I mice were purchased (The Jackson Laboratories, Bar Harbor, ME) or bred in-house. CB6F1/J neonates (6–7 days old) were obtained through timed breeding of BALB/c (female) and C57BL/6 (male) mice (The Jackson Laboratories).²⁶ Mice were bred and housed under specific pathogen-free (SPF) conditions at the Uniformed Services University (USU). Studies were approved by and adhered to the USU Institutional Animal Care and Use Committee (IACUC).

RSV virus modification and propagation

A recombinant version of RSV strain A2 was generated expressing the full-length ovalbumin (OVA) open reading frame from an additional gene inserted between the RSV G and F genes (Supplemental Fig. 1). The RSV A2 strain was propagated in HEp-2 as previously published.¹⁶ For RSV-ova, virus was filtered through a 100kDa filter (Amicon Ultra-15) to remove free OVA, which was confirmed by OVA ELISA (data not shown).

Measurement of viral titer by plaque assay

Lungs were frozen in MEM/10%FCS and stored at -80°C . Thawed lungs were homogenized using a GentleMACS dissociator (Miltenyi Biotec, Germany). Samples were centrifuged and the supernatants were inoculated on 80% confluent HEp-2 cell monolayers in 12-well plates and overlaid with 0.75% methyl cellulose. After incubation for 5 days at 37°C , infected HEp-2 were fixed with formalin and stained with hematoxylin and eosin. Plaques were counted and plotted as shown.

RSV infection

Mice were anesthetized using aerosolized isoflurane (3%) and infected intranasally with 2×10^6 plaque-forming units (PFU) of live ovalbumin-expressing RSV A2 (RSV-ova) or 1×10^6 PFU of unmodified RSV A2 (RSV-wt). Volume used to infect mice was adjusted for weight by dilution with PBS to provide 5–6 μl /gram of weight.

Murine cell isolation

Mice were euthanized with lethal intraperitoneal injection of pentobarbital (250mg/kg). Lungs and dLNs were collected in RPMI/10% FBS. Lung tissue was homogenized using a GentleMACS dissociator and filtered through $70\mu\text{m}$ filter. dLN were homogenized by manual disruption between frosted glass slides. Single cell suspensions were layered over Fico/lite-LM (Atlanta Biologicals, MD) at room temperature and centrifuged at $1250 \times g$ for 20 minutes. Mononuclear cells were isolated by extracting from the Ficoll layer and then washed twice in PBS.

Flow cytometry

Mouse cell suspensions were initially incubated with anti-CD16/32 (BD Biosciences, San Jose, CA) and normal mouse serum (Jackson ImmunoResearch, West Grove, PA) at 4°C for 10 min to prevent non-specific antibody binding. Cells were then stained with fluorochrome-conjugated antibodies and/or tetramers (detailed in Supplemental Table 1) at 4°C for 20 minutes. Human MCs, after stimulation, were stained with fluorochrome-conjugated antibodies (Supplemental Table 1) at 4°C for 20 minutes. Viability was determined with Fixable Viability Dye (Invitrogen, Carlsbad, CA). All antibodies used were titrated on cells of interest for individual lots. Cell acquisition was performed on BD-LSR-II and analyzed using FACS Diva software (BD Biosciences) and FlowJo (Version 9) (Tree Star, Inc, Ashland, OR).

DC-T cell co-cultures

Cells from the dLNs of RSV-ova infected mice (2 DPI) were isolated and stained as described above and the cDC1 population was sorted using a FACS Aria II machine (BD Biosciences). OT-I tg cells were isolated from the spleens of OT-I TCR transgenic mice using MACS CD8⁺ T cell negative selection kit (Miltenyi Biotec), stained with CFSE, and washed prior to co-culture. Sorted cDC1s were plated with T cells at the ratio of 1 DC:20 T cells, with no exogenous peptide, therefore, the only source of antigen was that acquired *in vivo* during RSV-ova infection. OT-I tg cells cultured with exogenous peptide in the absence

of APCs served as positive controls, and those receiving no stimuli served as negative controls. Cells were co-cultured for 3 days prior to analysis by flow cytometry.

***In vivo* blockade of costimulatory molecules**

Costimulatory molecule blockade was performed in adult mice with 50µg of blocking antibodies against CD86 (clone GL1) and CD80 (clone 16–10A1) at 1 DPI or 5 DPI, or CD40 (clone FGK4.5) at 1 DPI, and compared with responses in animals administered equivalent doses of isotype control antibodies at 1 DPI (Bio X cell, Lebanon, NH). All antibodies were injected in 100µl volume intraperitoneally (i.p.).

RNA-Seq analysis of antigen-presenting cDC1s

K^b-OVA⁺ cDC1s were sorted from the dLNs 2 DPI using FACS Aria II machine. The purity of sorted cells was verified as >90%. 4000 K^b-OVA enriched-cDC1s were collected in lysis buffer. Three biologic replicates per age group were submitted for RNA extraction, cDNA library construction, sequencing, and gene identification (Cofactor Genomics). Differentially expressed genes (DEG) were imported into Ingenuity Pathway Analysis (IPA) software (QIAGEN, Germany). The highest activated networks (high z-score) were identified.

IFN-I quantification and *in vivo* experiments

Lung and dLN tissues were dissociated in PBS or PBS/0.1% Triton, respectively, then centrifuged at 2500 rpm for 5 minutes and supernatants frozen at –80°C. IFN-I was quantified using mouse IFNα ELISA (limit of detection 125ng/ml) (PBL Assay Science, Piscataway, NJ) or mouse/human IFNβ ELISA (limit of detection 12.5pg/ml) (R&D). Total protein was quantified using Pierce BCA protein assay kit (Thermo Fisher Scientific, Rockville, MD). Tissue homogenates were diluted appropriately for the detected signals to fall within assay limits, and calculations were performed according to number of mice pooled or quantity of total protein detected per sample. Mice that received IFN-I were anesthetized using isoflurane (3%), and mouse IFNαA2 protein (10⁴ U, as previously published³²) or mouse IFNβ (indicated doses) (both from PBL Assay Science) was administered intranasally in PBS/0.1% BSA at 8- and 24-hours PI. Control mice received PBS/0.1% BSA intranasally at the same time points.

Mononuclear cells from human blood

Peripheral blood samples from adults were obtained from healthy volunteers at the National Institutes of Health (NIH) after informed consent with approval from the International Review Board (IRB) of the NIH (NIAID Protocol number 03-I-0263) and provided de-identified. Non-identifiable umbilical cord blood samples were obtained with the approval of the IRB of the Walter Reed National Military Medical Center (WRNMMC) (Protocol number WRNMMC-EDO-2018–0203). Umbilical cord blood was collected after delivery of the placenta into citrate-phosphate-dextrose solution (Sigma). Human blood was diluted in an equal volume of PBS and layered over Ficoll-Paque PREMIUM (GE Healthcare, Silver Spring, MD). MCs were isolated by centrifuging at 400×g for 30 minutes. MCs were washed twice and frozen in FCS/10% DMSO. On day of stimulation, MCs were thawed, washed, and rested in 48-well plates for 2 hours. Human IFNβ (PBL Assay Science) or

R848 (InvivoGen, San Diego, CA), was then added for stimulation at 37°C for 16–18 hours prior to analysis by flow cytometry.

Statistical analyses

Data were analyzed with GraphPad Prism and indicated statistical tests. Mean \pm SD are depicted (* $p < 0.05$, ** $p < 0.001$, *** $p < 0.0001$, **** $p < 0.00001$, ns=not statistically significant).

Supplementary Material

Refer to Web version on PubMed Central for supplementary material.

ACKNOWLEDGMENTS

We thank Kateryna Lund at the USU Biomedical Instrument Core (BIC) for flow cytometry assistance; and the USU Laboratory of Animal Medicine (LAM) for animal care. We appreciate the support of M. C. B. Florez, I. Gordon, G. Chen, N. Berkowitz and the CTC staff for providing human adult peripheral blood; and L. Criscione and K. Elmezzi, as well as, the entire obstetrics staff at WRNMMC for umbilical cord blood collection.

This work was supported by the USUHS Department of Pediatrics grant PED-86-3658. U.J.B. and L.Y. were supported by the Intramural Program of the National Institute of Allergy and Infectious Diseases of the National Institutes of Health. The opinions and assertions expressed herein are those of the authors and are not to be construed as reflecting the views of USUHS, the U.S. Air Force, the U.S. Army, U.S. Navy, the U.S. military at large, or the U.S. Department of Defense. Title 17 U.S.C. 105 provides that ‘Copyright protection under this title is not available for any work of the United States Government.’ Title 17 U.S.C. 101 defines a ‘United States Government work’ as a work prepared by a military service member or employee of the United States Government as part of that person’s official duties.

REFERENCES

1. Simon AK, Hollander GA, McMichael A. Evolution of the immune system in humans from infancy to old age. *Proc Biol Sci* 2015; 282(1821): 20143085. [PubMed: 26702035]
2. Marodi L Down-regulation of Th1 responses in human neonates. *Clin Exp Immunol* 2002; 128(1): 1–2. [PubMed: 11982583]
3. Gensollen T, Iyer SS, Kasper DL, Blumberg RS. How colonization by microbiota in early life shapes the immune system. *Science* 2016; 352(6285): 539–544. [PubMed: 27126036]
4. Drajac C, Laubret D, Riffault S, Descamps D. Pulmonary Susceptibility of Neonates to Respiratory Syncytial Virus Infection: A Problem of Innate Immunity? *J Immunol Res* 2017; 2017: 8734504. [PubMed: 29250560]
5. Yu JC, Khodadadi H, Malik A, Davidson B, Salles E, Bhatia J et al. Innate Immunity of Neonates and Infants. *Front Immunol* 2018; 9: 1759. [PubMed: 30105028]
6. Prendergast AJ, Klenerman P, Goulder PJ. The impact of differential antiviral immunity in children and adults. *Nat Rev Immunol* 2012; 12(9): 636–648. [PubMed: 22918466]
7. Lozano R, Naghavi M, Foreman K, Lim S, Shibuya K, Aboyans V et al. Global and regional mortality from 235 causes of death for 20 age groups in 1990 and 2010: a systematic analysis for the Global Burden of Disease Study 2010. *Lancet* 2012; 380(9859): 2095–2128. [PubMed: 23245604]
8. Lambert L, Sagfors AM, Openshaw PJ, Culley FJ. Immunity to RSV in Early-Life. *Front Immunol* 2014; 5: 466. [PubMed: 25324843]
9. Heidema J, Lukens MV, van Maren WW, van Dijk ME, Otten HG, van Vught AJ et al. CD8+ T cell responses in bronchoalveolar lavage fluid and peripheral blood mononuclear cells of infants with severe primary respiratory syncytial virus infections. *J Immunol* 2007; 179(12): 8410–8417. [PubMed: 18056387]

10. Welliver TP, Garofalo RP, Hosakote Y, Hintz KH, Avendano L, Sanchez K et al. Severe human lower respiratory tract illness caused by respiratory syncytial virus and influenza virus is characterized by the absence of pulmonary cytotoxic lymphocyte responses. *J Infect Dis* 2007; 195(8): 1126–1136. [PubMed: 17357048]
11. Jozwik A, Habibi MS, Paras A, Zhu J, Guvenel A, Dhariwal J et al. Erratum: RSV- specific airway resident memory CD8+ T cells and differential disease severity after experimental human infection. *Nat Commun* 2016; 7: 11011. [PubMed: 26957359]
12. Munir S, Hillyer P, Le Nouen C, Buchholz UJ, Rabin RL, Collins PL et al. Respiratory syncytial virus interferon antagonist NS1 protein suppresses and skews the human T lymphocyte response. *PLoS Pathog* 2011; 7(4): e1001336. [PubMed: 21533073]
13. Nakano H, Burgents JE, Nakano K, Whitehead GS, Cheong C, Bortner CD et al. Migratory properties of pulmonary dendritic cells are determined by their developmental lineage. *Mucosal Immunol* 2013; 6(4): 678–691. [PubMed: 23168837]
14. Plantinga M, Williams M, Vanheerswyngheles M, Deswarte K, Branco-Madeira F, Toussaint W et al. Conventional and monocyte-derived CD11b(+) dendritic cells initiate and maintain T helper 2 cell-mediated immunity to house dust mite allergen. *Immunity* 2013; 38(2): 322–335. [PubMed: 23352232]
15. Ruckwardt TJ, Malloy AM, Morabito KM, Graham BS. Quantitative and qualitative deficits in neonatal lung-migratory dendritic cells impact the generation of the CD8+ T cell response. *PLoS Pathog* 2014; 10(2): e1003934. [PubMed: 24550729]
16. Malloy AM, Ruckwardt TJ, Morabito KM, Lau-Kilby AW, Graham BS. Pulmonary Dendritic Cell Subsets Shape the Respiratory Syncytial Virus-Specific CD8+ T Cell Immunodominance Hierarchy in Neonates. *J Immunol* 2017; 198(1): 394–403. [PubMed: 27895172]
17. Bachus H, Kaur K, Papillion AM, Marquez-Lago TT, Yu Z, Ballesteros-Tato A et al. Impaired Tumor-Necrosis-Factor-alpha-driven Dendritic Cell Activation Limits Lipopolysaccharide-Induced Protection from Allergic Inflammation in Infants. *Immunity* 2019; 50(1): 225–240 e224. [PubMed: 30635238]
18. Williams M, Dutertre CA, Scott CL, McGovern N, Sichien D, Chakarov S et al. Unsupervised High-Dimensional Analysis Aligns Dendritic Cells across Tissues and Species. *Immunity* 2016; 45(3): 669–684. [PubMed: 27637149]
19. Helft J, Manicassamy B, Guernonprez P, Hashimoto D, Silvin A, Agudo J et al. Cross-presenting CD103+ dendritic cells are protected from influenza virus infection. *J Clin Invest* 2012; 122(11): 4037–4047. [PubMed: 23041628]
20. Porgador A, Yewdell JW, Deng Y, Bennink JR, Germain RN. Localization, quantitation, and in situ detection of specific peptide-MHC class I complexes using a monoclonal antibody. *Immunity* 1997; 6(6): 715–726. [PubMed: 9208844]
21. Obar JJ, Khanna KM, Lefrancois L. Endogenous naive CD8+ T cell precursor frequency regulates primary and memory responses to infection. *Immunity* 2008; 28(6): 859–869. [PubMed: 18499487]
22. Hickman HD, Mays JW, Gibbs J, Kosik I, Magadan JG, Takeda K et al. Influenza A Virus Negative Strand RNA Is Translated for CD8(+) T Cell Immunosurveillance. *J Immunol* 2018; 201(4): 1222–1228. [PubMed: 30012850]
23. Wu SW, Li L, Wang Y, Xiao Z. CTL-Derived Exosomes Enhance the Activation of CTLs Stimulated by Low-Affinity Peptides. *Front Immunol* 2019; 10: 1274. [PubMed: 31275303]
24. Wherry EJ, Puorro KA, Porgador A, Eisenlohr LC. The induction of virus-specific CTL as a function of increasing epitope expression: responses rise steadily until excessively high levels of epitope are attained. *J Immunol* 1999; 163(7): 3735–3745. [PubMed: 10490969]
25. Wu T, Guan J, Handel A, Tschärke DC, Sidney J, Sette A et al. Quantification of epitope abundance reveals the effect of direct and cross-presentation on influenza CTL responses. *Nat Commun* 2019; 10(1): 2846. [PubMed: 31253788]
26. Ruckwardt TJ, Malloy AM, Gostick E, Price DA, Dash P, McClaren JL et al. Neonatal CD8 T-cell hierarchy is distinct from adults and is influenced by intrinsic T cell properties in respiratory syncytial virus infected mice. *PLoS Pathog* 2011; 7(12): e1002377. [PubMed: 22144888]

27. Velilla PA, Rugeles MT, Chougnnet CA. Defective antigen-presenting cell function in human neonates. *Clin Immunol* 2006; 121(3): 251–259. [PubMed: 17010668]
28. Kollmann TR, Way SS, Harowicz HL, Hajjar AM, Wilson CB. Deficient MHC class I cross-presentation of soluble antigen by murine neonatal dendritic cells. *Blood* 2004; 103(11): 4240–4242. [PubMed: 14982880]
29. Steinman RM. Dendritic cells and the control of immunity: enhancing the efficiency of antigen presentation. *Mt Sinai J Med* 2001; 68(3): 160–166. [PubMed: 11373688]
30. Harding FA, McArthur JG, Gross JA, Raulet DH, Allison JP. CD28-mediated signalling co-stimulates murine T cells and prevents induction of anergy in T-cell clones. *Nature* 1992; 356(6370): 607–609. [PubMed: 1313950]
31. Kramer A, Green J, Pollard J Jr., Tugendreich S Causal analysis approaches in Ingenuity Pathway Analysis. *Bioinformatics* 2014; 30(4): 523–530. [PubMed: 24336805]
32. Cormier SA, Shrestha B, Saravia J, Lee GI, Shen L, DeVincenzo JP et al. Limited type I interferons and plasmacytoid dendritic cells during neonatal respiratory syncytial virus infection permit immunopathogenesis upon reinfection. *J Virol* 2014; 88(16): 9350–9360. [PubMed: 24920801]
33. Montoya M, Schiavoni G, Mattei F, Gresser I, Belardelli F, Borrow P et al. Type I interferons produced by dendritic cells promote their phenotypic and functional activation. *Blood* 2002; 99(9): 3263–3271. [PubMed: 11964292]
34. Barik S Respiratory syncytial virus mechanisms to interfere with type I interferons. *Curr Top Microbiol Immunol* 2013; 372: 173–191. [PubMed: 24362690]
35. Breton G, Lee J, Zhou YJ, Schreiber JJ, Keler T, Puhf S et al. Circulating precursors of human CD1c+ and CD141+ dendritic cells. *J Exp Med* 2015; 212(3): 401–413. [PubMed: 25687281]
36. Lund JM, Alexopoulou L, Sato A, Karow M, Adams NC, Gale NW et al. Recognition of single-stranded RNA viruses by Toll-like receptor 7. *Proc Natl Acad Sci U S A* 2004; 101(15): 5598–5603. [PubMed: 15034168]
37. Levy O, Zarembek KA, Roy RM, Cywes C, Godowski PJ, Wessels MR. Selective impairment of TLR-mediated innate immunity in human newborns: neonatal blood plasma reduces monocyte TNF-alpha induction by bacterial lipopeptides, lipopolysaccharide, and imiquimod, but preserves the response to R-848. *J Immunol* 2004; 173(7): 4627–4634. [PubMed: 15383597]
38. Hijano DR, Siefker DT, Shrestha B, Jaligama S, Vu LD, Tillman H et al. Type I Interferon Potentiates IgA Immunity to Respiratory Syncytial Virus Infection During Infancy. *Sci Rep* 2018; 8(1): 11034. [PubMed: 30038294]
39. Malloy AM, Falsey AR, Ruckwardt TJ. Consequences of immature and senescent immune responses for infection with respiratory syncytial virus. *Curr Top Microbiol Immunol* 2013; 372: 211–231. [PubMed: 24362692]
40. Adkins B, Leclerc C, Marshall-Clarke S. Neonatal adaptive immunity comes of age. *Nat Rev Immunol* 2004; 4(7): 553–564. [PubMed: 15229474]
41. Kollmann TR. Variation between Populations in the Innate Immune Response to Vaccine Adjuvants. *Front Immunol* 2013; 4: 81. [PubMed: 23565115]
42. Gold MC, Robinson TL, Cook MS, Byrd LK, Ehlinger HD, Lewinsohn DM et al. Human neonatal dendritic cells are competent in MHC class I antigen processing and presentation. *PLoS One* 2007; 2(9): e957. [PubMed: 17895997]
43. Dadaglio G, Sun CM, Lo-Man R, Siegrist CA, Leclerc C. Efficient in vivo priming of specific cytotoxic T cell responses by neonatal dendritic cells. *J Immunol* 2002; 168(5): 2219–2224. [PubMed: 11859108]
44. Teijaro JR. Type I interferons in viral control and immune regulation. *Curr Opin Virol* 2016; 16: 31–40. [PubMed: 26812607]
45. Hall CB, Douglas RG, Jr., Simons RL, Geiman JM. Interferon production in children with respiratory syncytial, influenza, and parainfluenza virus infections. *J Pediatr* 1978; 93(1): 28–32. [PubMed: 206677]
46. Koga Y, Matsuzaki A, Suminoe A, Hattori H, Hara T. Expression of cytokine-associated genes in dendritic cells (DCs): comparison between adult peripheral blood- and umbilical cord blood-derived DCs by cDNA microarray. *Immunol Lett* 2008; 116(1): 55–63. [PubMed: 18192028]

47. Rahman MJ, Rodrigues KB, Quiel JA, Liu Y, Bhargava V, Zhao Y et al. Restoration of the type I IFN-IL-1 balance through targeted blockade of PTGER4 inhibits autoimmunity in NOD mice. *JCI Insight* 2018; 3(3).
48. Bonifaz L, Bonnyay D, Mahnke K, Rivera M, Nussenzweig MC, Steinman RM. Efficient targeting of protein antigen to the dendritic cell receptor DEC-205 in the steady state leads to antigen presentation on major histocompatibility complex class I products and peripheral CD8+ T cell tolerance. *JExp Med* 2002; 196(12): 1627–1638. [PubMed: 12486105]
49. Rice GI, Kasher PR, Forte GM, Mannion NM, Greenwood SM, Szykiewicz M et al. Mutations in ADAR1 cause Aicardi-Goutieres syndrome associated with a type I interferon signature. *Nat Genet* 2012; 44(11): 1243–1248. [PubMed: 23001123]
50. Liu Y, Qu L, Liu Y, Roizman B, Zhou GG. PUM1 is a biphasic negative regulator of innate immunity genes by suppressing LGP2. *Proc Natl Acad Sci U S A* 2017; 114(33): E6902–E6911. [PubMed: 28760986]

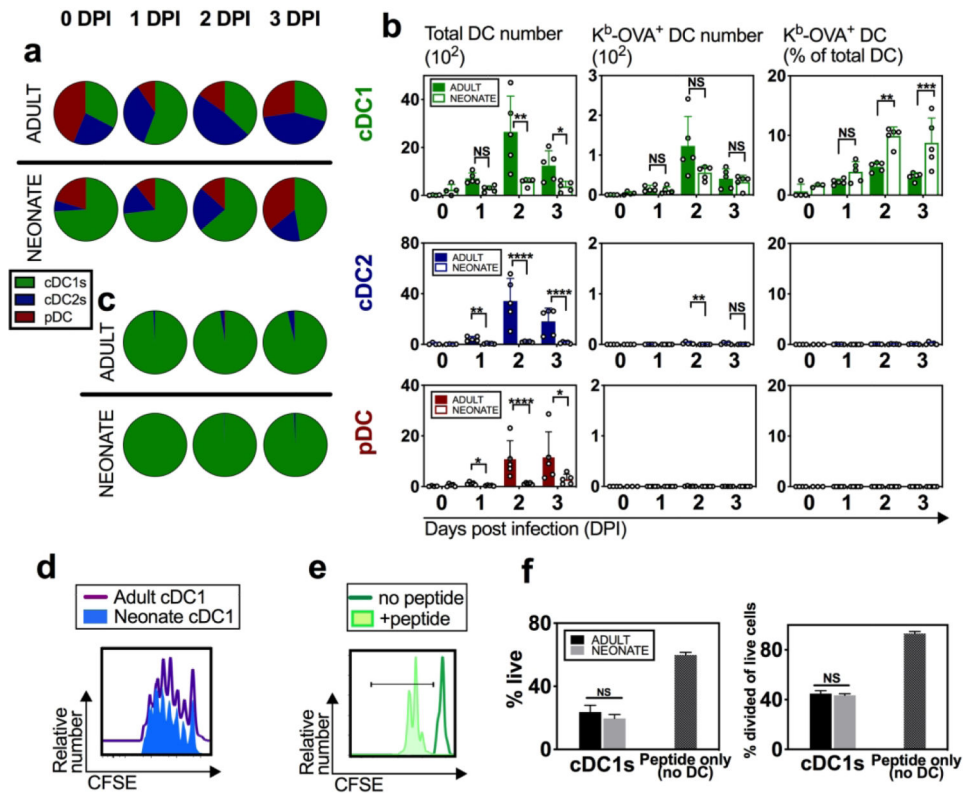


Fig. 1. Neonatal cDC1s can efficiently present RSV-ova derived antigen at the site of CD8⁺ T cell priming.

Adult and neonatal mice were intranasally infected with RSV-ova and specific DC subsets were identified from the lung-draining mediastinal lymph nodes (dLNs) on indicated day(s) post infection (DPI). **a** Pies represent the relative proportion of the three DC subsets based on cell count per dLN on indicated DPI. **b** Number and percentage of total DC population or K^b-OVA⁺ DCs per dLN on indicated DPI. **c** Pies represent the relative proportion of K^b-OVA⁺ DCs based on cell count per dLN on indicated DPI. **d** Histogram of CFSE dilution resulting from proliferation of OT-I tg cells exposed to cDC1s sorted from the dLN of RSV-ova-infected adult or neonatal mice at 2 DPI. **e** Histogram of CFSE dilution of proliferating OT-I tg cells exposed to SIINFEKL peptide alone without APCs, or unstimulated. **f** Quantitative measurements of OT-I tg cell viability and proliferation in response to experimental conditions in d and e. Data are representative of three independent experiments showing similar results. **a-c** 4–5 samples per group and 2–8 dLN pooled per sample. Cell number is determined by running the sample to completion and dividing by number of pooled dLNs. **d, e, f** dLN from 10 mice pooled to sort cDC1s for replicate co-cultures. Mean \pm SD are depicted (* $p < 0.05$, ** $p < 0.001$, *** $p < 0.0001$, **** $p < 0.00001$, NS=not statistically significant). **b** Two-way ANOVA with Sidak's multiple comparisons test (after normalizing to log scale to correct for variance). **f** Multiple t-tests with Benjamini and Hochberg FDR.

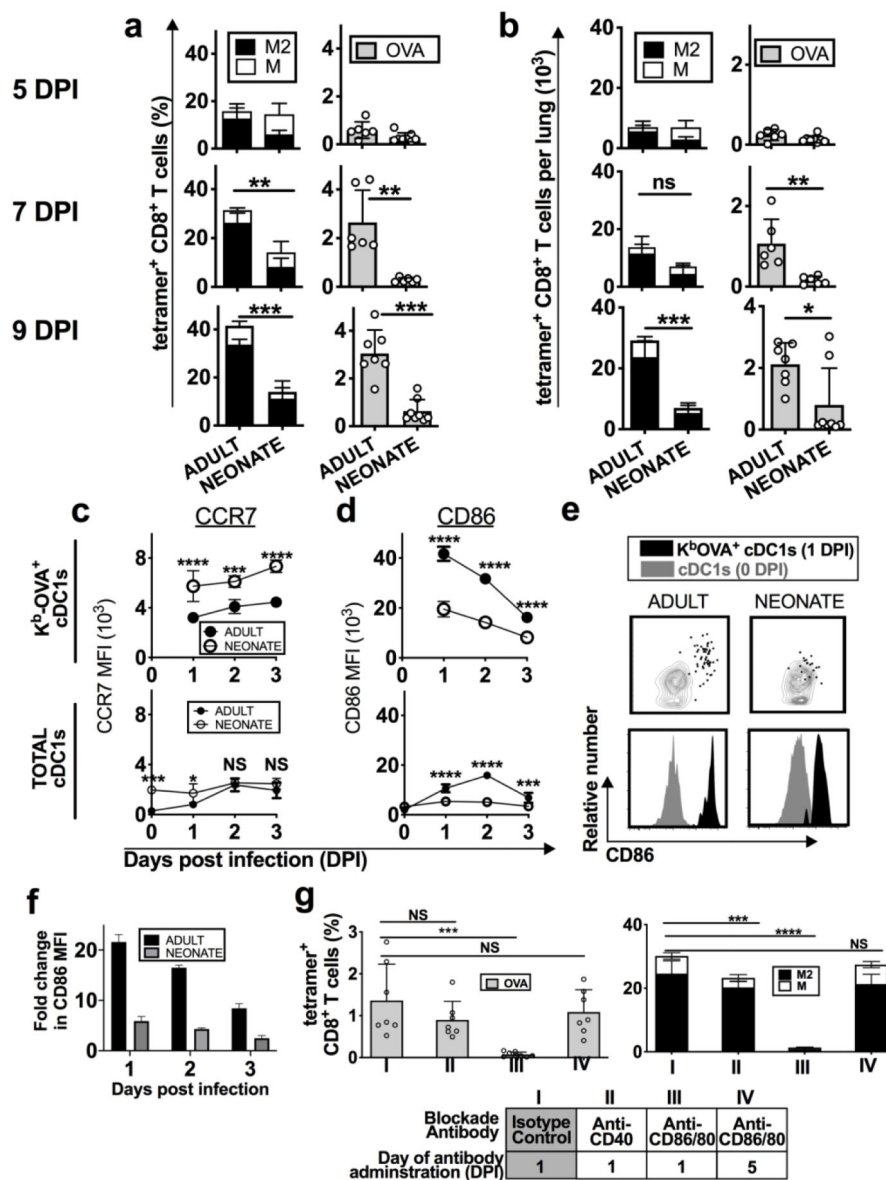


Fig. 2. Reduced anti-RSV-ova specific CD8⁺ T cell responses were associated with dysfunctional activation of neonatal cDC1s.

Adult and neonatal mice were infected with RSV-ova **a, b** RSV-ova-specific CD8⁺ T cell responses in the lungs were measured with MHC-I tetramer at 5, 7, and 9 DPI for K^dM2₈₂₋₉₀, D^bM₁₈₇₋₁₉₅ and K^bOVA₂₅₇₋₂₆₄ restricted epitopes, and quantified as **a** percentage of total CD8⁺ T cells or **b** number per lung. **c, d** Cells were isolated from dLNs at indicated days post infection and expression of **c** CCR7 and **d** CD86 was measured by MFI on K^b-OVA⁺ (*top*) or total cDC1s (*bottom*). **e** Expression of CD86 on cDC1s from the dLN 0 DPI (steady-state mice) (*grey*) or on K^b-OVA⁺ cDC1s 1 DPI (*black*) is shown as dot plots and histograms. **f** Fold change in MFI of CD86, measured on K^b-OVA⁺ cDC1s isolated from the dLN at indicated DPI, above the CD86 MFI measured on naive steady-state cDC1s from respective age group. **g** RSV-ova-specific CD8⁺ T cells measured 7 DPI, after *in vivo*

blockade of CD86/80 or CD40 with monoclonal blocking antibodies (mAb) against the respective costimulatory molecule via intraperitoneal injection at indicated DPI in adult mice. Isotype control antibodies were administered 1 DPI. Data are representative of two-three independent experiments showing similar results. **a, b, g** one mouse per sample, 4–5 samples per group. **c, d, f** 2–8 mice pooled per sample, 5 samples per group. Mean \pm SD are depicted (* $p < 0.05$, ** $p < 0.001$, *** $p < 0.0001$, **** $p < 0.00001$). **a, b** Mann-Whitney *U* test. **c, d** Two-way ANOVA with Sidak's multiple comparisons test. **g** One-way ANOVA with Dunnett's multiple comparisons.

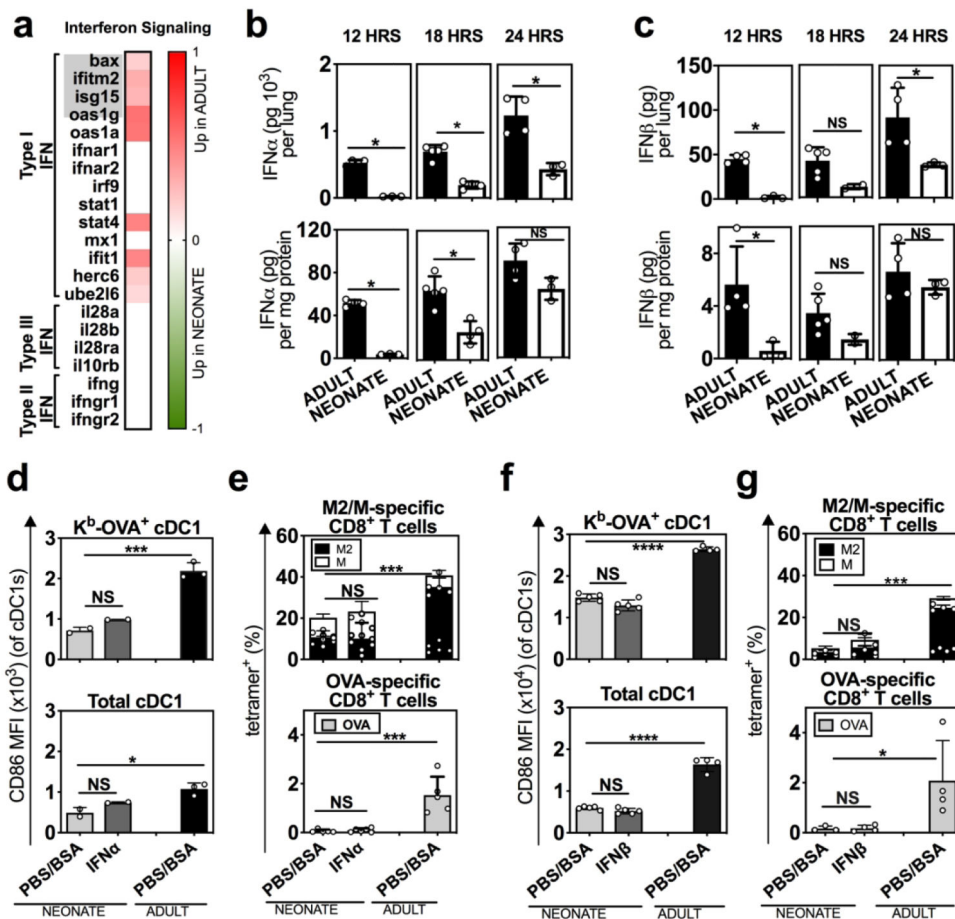


Fig. 3. Neonatal mice exhibited reduced IFN-I production, but also restricted responsiveness to IFN-I by cDC1s during RSV infection.

a K^b-OVA⁺ cDC1s from the dLN of RSV-ova infected adult and neonatal mice were enriched by sorting, and analyzed using RNA-seq to identify DEG (red and green shaded genes). Heat map showing the log fold change (Log_{FC}) of adult compared to neonatal interferon signaling genes. The top five genes, indicated in grey, were identified by IPA to define a difference in the interferon signaling pathway between neonates and adults. Additional genes are shown to provide further context for the different IFN signaling genes.

b, c Quantification of **b** IFN α or **c** IFN β by ELISA from neonatal and adult lungs at indicated hours PI. **d, e** Effect of intranasal IFN α (10^4 U at 8- and 24-hours PI) on the **d** expression of CD86 on neonatal cDC1s from the dLN 2 DPI and **e** neonatal RSV-ova-specific CD8⁺ T cells 7 DPI from the lung. **f, g** Effect of intranasal IFN β (10^3 U at 8- and 24-hours PI) on **f** expression of CD86 on neonatal cDC1s from the dLN 2 DPI and **g** neonatal RSV-ova-specific CD8⁺ T cells 7 DPI from the lung. **b, c, d, f** Data are representative of three independent experiments showing similar results, 4–6 samples per group, 2–8 mice pooled per sample. **e, g** one mouse per sample, 4–5 samples per group. Mean \pm SD are depicted (* $p < 0.05$, ** $p < 0.001$, *** $p < 0.0001$, **** $p < 0.00001$). **b, c** Mann-Whitney *U* test. **d-g** One-way ANOVA with Tukey's multiple comparison test.

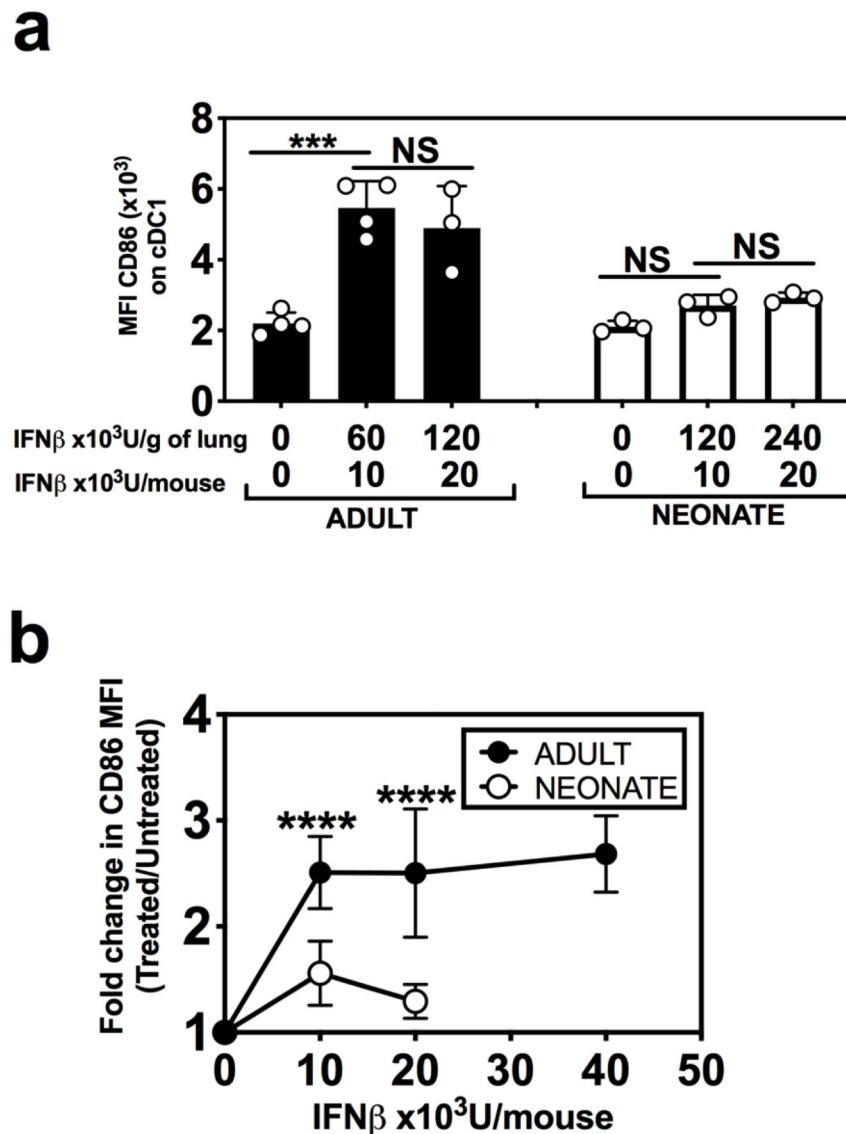


Fig. 4. Neonatal cDC1s exhibit reduced responsiveness to IFN-I.

Naïve adult and neonatal mice were administered the indicated doses of intranasal IFN β . **a**, Expression of CD86 was measured on cDC1s isolated from the lung at 18–20 hours post intranasal IFN β administration. Data are shown as **a** MFI of CD86 expression and **b** fold-changes in MFI of CD86 expression compared to untreated. Data are representative of at least three independent experiments showing similar results. 3–4 samples per group, 2–8 mice were pooled per sample. **b** represents data from five different experiments normalized by using fold change comparing treated to controls (PBS+BSA treated). Mean \pm SD are depicted (* $p < 0.05$, ** $p < 0.001$, *** $p < 0.0001$, **** $p < 0.00001$). **a** One-way ANOVA with Tukey's multiple comparison test. **b** Two-way ANOVA with Sidak's multiple comparisons test.

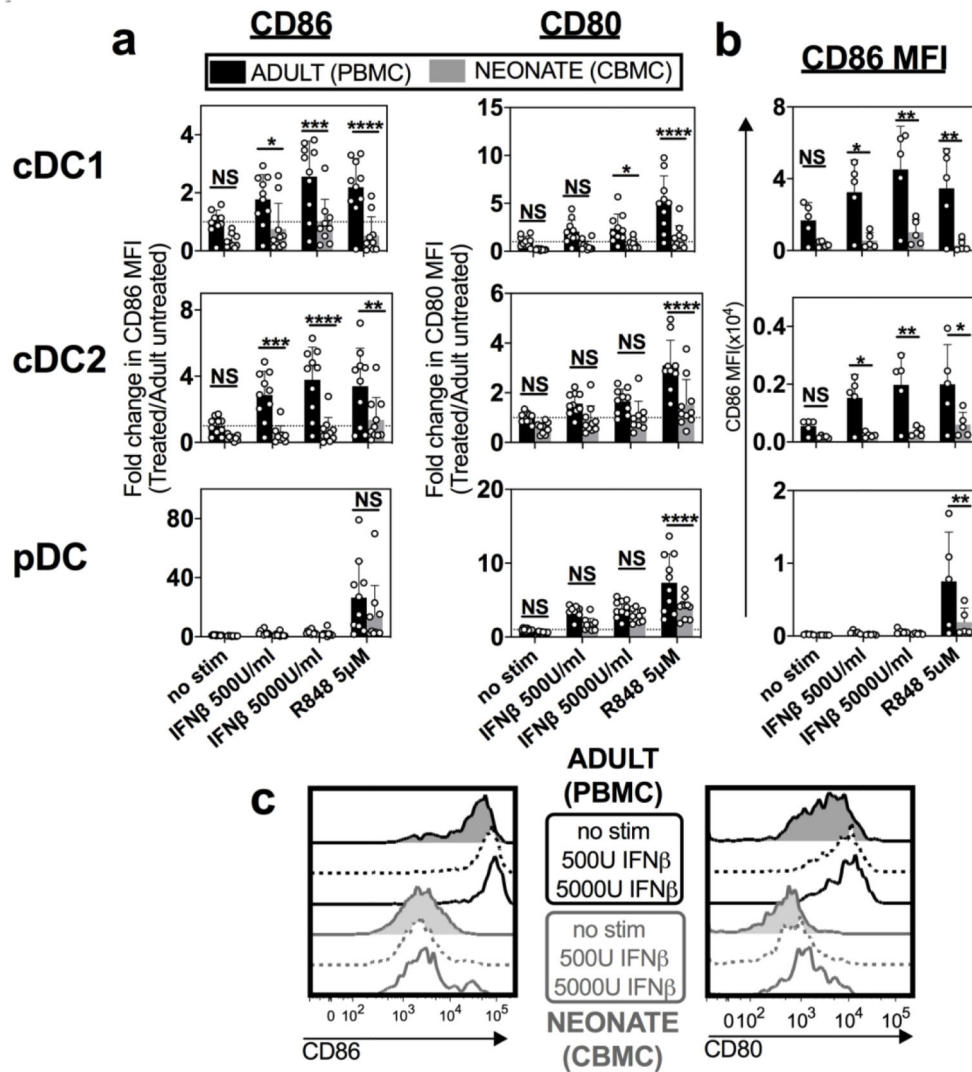


Fig. 5. Human neonatal cDC1s also exhibited limited upregulation of costimulatory molecule expression in response to IFN-I.

Mononuclear cells were isolated from human adult peripheral blood (Adult, PBMC) and umbilical cord blood (Neonate, CBMC) and stimulated *in vitro* with indicated stimuli (human IFN β or R848). **a** Fold change of CD86 and CD80 MFI relative to unstimulated adult PBMCs is represented for three different DC subsets: cDC1, cDC2 and pDC. **b** MFI of CD86 used to calculate fold change, shown for each treatment condition and DC subset. **c** Representative histograms of CD86 and CD80 expression on neonatal and adult cDC1s comparing unstimulated with IFN β stimulated cells at indicated doses. Data are representative of three independent experiments showing similar results. Mean \pm SD are depicted, (* $p < 0.05$, ** $p < 0.001$, *** $p < 0.0001$, **** $p < 0.00001$). **a, b** Two-way ANOVA was used with Sidak's multiple comparisons test.